International Journal of GEOMATE, Dec., 2020, Vol.19, Issue 76, pp. 126–133
ISSN: 2186-2982 (P), 2186-2990 (O), Japan, DOI: https://doi.org/10.21660/2020.76.42744
Special Issue on Science, Engineering and Environment

WAVE GENERATION ON AN INCLINED OPEN CHANNEL WITH A BUMP

*Ikha Magdalena[1] and Leo Hari Wiryanto[1]

[1]Industrial and Financial Mathematical Research Group, Faculty of Mathematics and Natural Sciences, Institut Teknologi Bandung, Indonesia.

*Corresponding Author, Received: 17 April 2020, Revised: 06 May 2020, Accepted: 15 Aug. 2020

ABSTRACT: A uniform flow on an open channel is studied in this paper. Shallow water equations are used as the model by involving the bottom topography. In this problem, we focus on incline bottom and put a bump on it, so that the flow generates a surface wave. The model is extended by energy dissipation through tangential shear and the energy dissipation by shearing normal to the flow. In non-dimensional variables, the profile of the fluid surface is observed as waves growing to split and propagating, depending on the type of the bump, parameters angle of the channel, Froude number and Reynolds number. When the angle is not zero, we found that the waves propagate downward and possible appearing secondary waves or undular bore, that does not occur for zero angles but agrees to the model of Boussinesq equations. To get the accurate result with purely showing the damping effect from the equation, the finite volume method has been applied on a staggered grid that is free from damping error to solve the equations numerically.

Keywords: Shallow water equations, Froude number, Reynolds number, Undular bore.

1. INTRODUCTION

A uniform flow disturbed by an obstruction can generate wave on the surface. The obstruction can be a bump on the bottom of a channel. The wave grows, splits and propagates starting from above the obstruction. Those generated waves can be destructive for both waterway banks and nearby infrastructures. Understanding the characteristics of the generated surface wave is very important to determine the best way to protect the banks and infrastructures around the channel. Wiryanto and Mungkasi [1] modeled the phenomena by Boussinesq equations to perform the wave generation and to confirm the stable solution obtained from a steady Korteweg de Vries model in [2,3]. The model of Korteweg de Vries equation containing a forcing term gives two solutions for given a bump and the strength of the uniform flow presented as Froude number $\boldsymbol{F}$. The solution that can be happened in the real situation is a question that was wanted to be answered in [1]. Moreover, their model can simulate the wave generation for a subcritical flow that is not obtained in the steady model.

On the other hand, Shallow Water Equations (SWEs) are another model that can simulate wave propagation, also wave generation. The derivation of SWEs can be seen in [4] based on control volume of mass and momentum conservations. Wiryanto [5] studied that model to observe the effect of a sloping bottom of the channel and involving the bottom friction. Traveling wave is one of the solution types that can be obtained for a particular condition, i.e. the velocity is proportional to the square of the fluid depth that is then called as the kinematic wave. Numerically, Wiryanto [5] indicated that the kinematic wave could be obtained for $\boldsymbol{F = 2}$, and for $\boldsymbol{F > 2}$ the surface elevation increases by increasing time. The results confirm to [6,7]. Besides Dressler and Needham & Merkin, Que & Xu [8] showed numerically the existence of a periodic wave describing phenomena called roll wave as the effect of the bottom friction. The phenomena do not occur when the friction term is neglected, such discussed in [9]. To obtain roll wave phenomena, the initial condition is required in solving the model. This paper provides the initial wave for that phenomena by considering wave generation and extends the model in [1]. Fluid flows uniformly on an inclined channel and is disturbed by a bump. Therefore, the free surface wave performs elevation as the wave propagating downward. Model in [7] is adopted by involving a bump. The adopted model has been verified by a comparison between its numerical and analytical solution. The numerical solution is obtained using Runge-Kutta Method, while the analytical solution is obtained by applying the Hopf bifurcation theorem which then uniformly expanded using Krylov-Bogoliubov-Mitropolski averaging method. In case the slope of the channel is flat, the result confirms to [1], and wave with undular bore appears far from the disturbance, for sloping bottom $\boldsymbol{\theta > 0}$ and for $\boldsymbol{1 < F < 1.7}$. In this research, the most important and challenging part is we need a

numerical scheme that is able to study the damping effect caused by the diffusive terms only. Therefore, we derived numerical scheme based on finite volume method that is free from damping error.

There are five sections in this paper. The first section introduces the proposed numerical model. The governing equations are briefly introduced in the second section. In the following section, a staggered finite volume method is described. In the fourth section, numerical results are presented for validation of uniform flow case and followed with a simulation of wave generation over a bump for a sub and supercritical flow. The formation of the undular bore is shown in the numerical result section. Conclusions are outlined in the last section.

2. SHALLOW WATER EQUATIONS OVER AN INCLINED CHANNEL

Physically, we consider a model of a uniform stream of velocity u_0 and undisturbed water depth h_0. The stream is on an inclined channel of angle θ. We choose the horizontal x-axis along the bottom and the vertical y-axis is perpendicular to the horizontal axis, so that the bottom topography is $y = b(x)$, ilustrated in Fig.1. We use notation $g_x = g\sin\theta$ and $g_y = g\cos\theta$ representing the gravity in x and y direction.

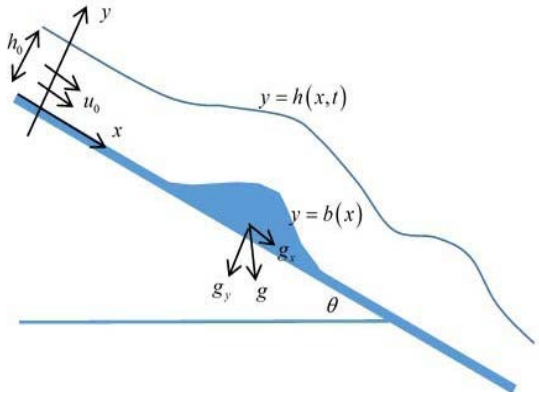

Fig.1 Sketch of the flow and coordinates.

The existing of a bump on the bottom of the channel effects the stream so that the free surface becomes $h(x,t) = h_0 + a(x,t)$ with $a(x,t)$ is the surface elevation that is calculated from h_0. The average depth velocity is denoted by $u(x,y)$. Those quantities satisfy

$$\begin{aligned} &\frac{\partial h}{\partial t} + \frac{\partial (h-b)u}{\partial x} = 0 \\ &\frac{\partial u}{\partial t} + u\frac{\partial u}{\partial x} + g_y\frac{\partial (h-b)}{\partial x} \\ &\qquad = g_y S - C_f\frac{|u|u}{h-b} + \nu_0\frac{\partial^2 u}{\partial x^2}, \end{aligned} \tag{1}$$

where $S = \tan\theta$ is the tangential of the bottom, and C_f is the roughness of the bottom of the channel. The term containing the constant ν_0 represents the energy dissipation effected by shearing normal to the flow. We use the shallow water equations following [7] by involving a bump $y = b(x)$. The first equation relates to mass conservation law, and the second one is momentum balance. The equations can be derived by control volume such as extending the procedure in [4,5]. These are given in Appendix of this paper.

In solving Eq. (1), we first consider constant solution given by uniform stream for small bump. Thus, the second equation of Eq. (1) gives us the relation between h_0 and u_0 read as

$$u_0^2 = \frac{g_y S}{C_f} h_0. \tag{2}$$

Based on this solution we rewrite the Eq. (1) in non-dimensional variables by introducing new notations

$$\eta = \frac{h}{h_0}, \bar{a} = \frac{a}{h_0}, w = \frac{u}{u_0},$$
$$\xi = \frac{x}{l}, \tau = \frac{u_0}{l}t, d = \frac{b}{h_0}$$

so that the first equation of Eq. (1) becomes

$$\frac{\partial \eta}{\partial \tau} + \frac{\partial w(\eta - d)}{\partial \xi} = 0, \tag{3}$$

and the second equation of Eq. (1) becomes

$$\begin{aligned} \frac{\partial w}{\partial \tau} + w\frac{\partial w}{\partial \xi} + \frac{1}{F^2}\left(\frac{\partial \eta}{\partial \xi} - d'\right) \\ = \frac{S}{\epsilon F^2}\left(1 - \frac{w|w|}{\eta - d}\right) \\ + \frac{1}{Re}\frac{\partial^2 w}{\partial \xi^2}. \end{aligned} \tag{4}$$

Eq. (4) contains two parameters $F = u_0/\sqrt{g_y h_0}$ as Froude number and $Re = u_0 l/\nu_0$ as Reynold number. We also use l as the horizontal scale, and ϵ is small value defined as the ratio between uniform depth h_0 and l. From Eq. (2) we can express C_f in terms of Froude number F as $C_f = S/F^2$.

3. NUMERICAL PROCEDURE

In this section, we will formulate a numerical scheme to solve Eqs. (3,4) numerically. Finite volume on a staggered grid is applied here. Working with finite volume on a staggered grid gives us an advantage where we can ignore solving the Riemann problem as a standard finite volume

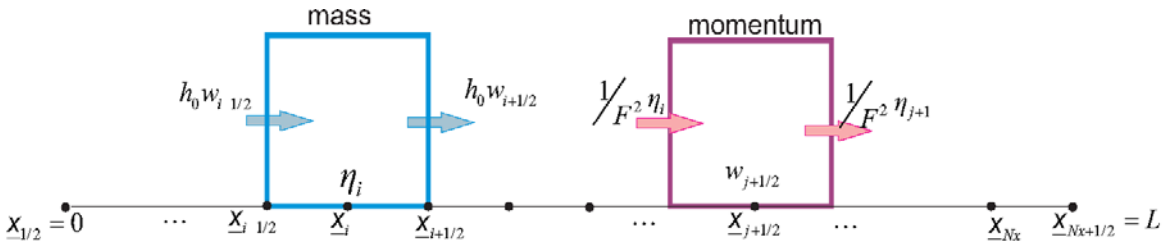

method does.

Fig2 Illustration of staggered grid with cell $[\boldsymbol{\xi_{i-1/2}, \xi_{i+1/2}}]$ for mass conservation and cell $[\boldsymbol{\xi_{i-1}, \xi_i}]$ for momentum equation.

Consider non-dimensional Eqs. (3,4) in a computational domain $[0, L]$. We discretize the domain in a staggered way $0 = \xi_{1/2}, \xi_1, \dots, \xi_{Nx+1/2} = L$. Mass conservation, i.e. Eq. (3) is approximated at a cell centered at ξ_i whereas momentum conservation, i.e. Eq. (4) is approximated at a cell centered at $\xi_{i+1/2}$, (Fig.2) In this setting, values of η will be computed at every full grid points ξ_i, with $i = 1,2,\dots,Nx$ using mass conservation, i.e. Eq. (5). Velocity w will be computed at every staggered grid points $\xi_{i+\frac{1}{2}}$, with $i = 1,2,\dots,Nx-1$ using momentum equation, i.e. Eq. (6). Approximate equations are then

$$\frac{\boldsymbol{\eta_i^{n+1} - \eta_i^n}}{\boldsymbol{\Delta\tau}} + \frac{(^*\boldsymbol{(hh)w})^n_{i+\frac{1}{2}} - (^*\boldsymbol{(hh)w})^n_{i-1/2}}{\boldsymbol{\Delta\xi}} = \mathbf{0}, \tag{5}$$

$$\frac{\boldsymbol{w^{n+1}_{i+\frac{1}{2}} - w^n_{i+\frac{1}{2}}}}{\boldsymbol{\Delta\tau}} + \boldsymbol{\left(ww_\xi\right)^n_{i+\frac{1}{2}}} + \frac{\mathbf{1}}{\boldsymbol{F^2}}\frac{\boldsymbol{(hh)^{n+1}_{i+1} - (hh)^{n+1}_i}}{\boldsymbol{\Delta\xi}} = \frac{\boldsymbol{S}}{\boldsymbol{\epsilon F^2}}\left(\mathbf{1} - \frac{\boldsymbol{|w|^n_{i+1/2} w^{n+1}_{i+1/2}}}{\boldsymbol{\overline{hh}_{i+1/2}}}\right) + \frac{\mathbf{1}}{\boldsymbol{R_e}}\frac{\boldsymbol{\partial^2 w}}{\boldsymbol{\partial\xi^2}}, \tag{6}$$

where $hh = \eta - d$. In Eq. (5), the values of hh in a half grid are undefined, terms are indicated by the superscript *. We approximate their values using the first-order upwind method:

$$^*\boldsymbol{(hh)}_{i+\frac{1}{2}} = \begin{cases} \boldsymbol{(hh)_i}, & \boldsymbol{if \quad w_{i+1/2} \geq 0}, \\ \boldsymbol{(hh)_{i+1}}, & \boldsymbol{if \quad w_{i+1/2} < 0}. \end{cases} \tag{7}$$

In a friction terms is approximated by Picard linearization, read as $\frac{|w|^n_{i+1/2} w^{n+1}_{i+1/2}}{\overline{hh}_{i+1/2}}$ with

$$\boldsymbol{\overline{(hh)}_{i+1/2} \simeq \frac{1}{2}((hh)_{i+1} + (hh)_{i-1})}.$$

The diffusive term in the right hand side is discritized by

$$\frac{\mathbf{1}}{\boldsymbol{R_e}}\frac{\boldsymbol{\partial^2 w}}{\boldsymbol{\partial\xi^2}} = \frac{\mathbf{1}}{\boldsymbol{R_e}}\frac{\boldsymbol{w_{i+3/2} - 2w_{i+1/2} + w_{i-1/2}}}{\boldsymbol{\Delta\xi^2}}.$$

The difficulty in the equation is in approximating the advection term $(ww_\xi)_{i+1/2}$. We approximate the advection term using this relation

$$\boldsymbol{ww_\xi = \frac{1}{hh}\left(\frac{\partial(qw)}{\partial\xi} - w\frac{\partial q}{\partial\xi}\right)}, \tag{8}$$

where $q = (hh)w$ denotes the horizontal momentum. Thus under the condition that the average of total water depth remains positive $\overline{hh}_{i+1/2} > 0$, the advection term in Eq. (8) is approximated by

$$\boldsymbol{(ww_\xi)_{i+1/2}} = \frac{\mathbf{1}}{\boldsymbol{\overline{hh}_{i+\frac{1}{2}}}}\left(\frac{\boldsymbol{\overline{q}_{i+1} * w_{i+1} - \overline{q}_i * w_i}}{\boldsymbol{\Delta\xi}} - \boldsymbol{w_{i+\frac{1}{2}}}\frac{\boldsymbol{\overline{q}_{i+1} - \overline{q}_i}}{\boldsymbol{\Delta\xi}}\right), \tag{9}$$

$$\overline{hh}_{i+1/2} = \frac{1}{2}(hh_i + hh_{i+1}),$$

$$\bar{q}_i = \frac{1}{2}\left(q_{i+\frac{1}{2}} + q_{i-\frac{1}{2}}\right), \quad q_{i+\frac{1}{2}} = {}^*hh_{i+\frac{1}{2}} u_{i+\frac{1}{2}}.$$

At points denoted by $\boldsymbol{i}$ there is no value of $\boldsymbol{w}$, therefore it is indicated by $^*\boldsymbol{w_i}$ and approximated by

$$^*\boldsymbol{w_i} = \begin{cases} \boldsymbol{w_{i-\frac{1}{2}}}, & \boldsymbol{if\ \bar{q}_i \geq 0}, \\ \boldsymbol{w_{i+\frac{1}{2}}}, & \boldsymbol{if\ \bar{q}_i < 0}. \end{cases} \tag{10}$$

Thus this choice similarly depends on the flow direction, similar as the approximation of $^*\boldsymbol{hh}$ via

Eq. (7), and for positive flow the approximation for the advection is

$$\frac{\bar{q}_i}{\overline{hh}_{i+1/2}}\left(\frac{w_{i+\frac{1}{2}}-w_{i-\frac{1}{2}}}{\Delta\xi}\right) = \frac{hh_i w_{i+\frac{1}{2}}+hh_{i-1}w_{i-\frac{1}{2}}}{hh_i+hh_{i+1}}\left(\frac{w_{i+\frac{1}{2}}-w_{i-\frac{1}{2}}}{\Delta\xi}\right).$$

In case of flat bottom case, implementing Von Neumann stability analysis, we obtain stability condition for Eq. (5,6) which is $\sqrt{\frac{h_0}{F^2}}\frac{\Delta\tau}{\Delta\xi} \leq \mathbf{1}$, where h_0 is the undisturbed water depth. Note the friction term is calculated implicitly in order to avoid more restricted stability condition. In case fully nonlinear friction term used, then discrete form of $|w|w$ is $w^n w^{n+1}$ by implementing Picard linearization. The resulting scheme is free from numerical damping error, see [10] for details. Moreover, this numerical scheme successfully solve many application problems, such as written in [11-13].

4. NUMERICAL RESULTS

The numerical procedure described above can calculate the model for various values of parameters F and Re, but mainly our numerical calculations use $\epsilon = 0.1$. For all calculation, we choose the following discretization: $\Delta\xi = 0.1$ and $\Delta\tau = 0.01$. To validate our numerical scheme, we do a test case for uniform flow over an inclined channel. After the validation, we implement our numerical scheme to investigate flow over a bump on an inclined channel for various setting of slope θ, Froude F, and Reynolds number Re.

4.1 Uniform Flow over an Inclined Channel

In this subsection, we consider uniform flow case over an inclined channel without a bump $d = 0$. In uniform flow, the gravity force is balanced with the drag force. We first consider a constant solution given by uniform stream over an inclined channel. Solving Eq. (3) will give us the relation between w_0 and η written as

$$w_0^2 = \eta = 1 + \bar{a}. \quad (11)$$

If $\bar{a} = 0$ then $w = w_0 = 1$, and it describes a river flowing uniformly down to the sea without any waves or disturbances. Substituting Eq. (11) into the first equation of Eq. (3) yields

$$\eta_\tau + (G(\eta))_\xi = 0, with\ G(\eta) = (\eta)^{3/2} \quad (12)$$

A shock wave governed by Eq. (12) moves with phase velocity according to the Rankine Hugoniot condition

$$phasevelocity = \frac{[G(\eta)]}{[\eta]} = \frac{(\eta_l)^{3/2}-(\eta_r)^{3/2}}{(\eta_l-\eta_r)}. \quad (13)$$

In the above formula, η_l and η_r are the left and right limiting values of the initial wave at the point of discontinuity. Here we apply our scheme as written in Eq. (5). Fig.3 shows numerical simulation of two cases starting from uniform initial condition $\eta(\xi,0) = 1$ and $w(\xi,0) = \sqrt{\eta(\xi,0)}$. Fig.3 simulates a sudden discharge comes from the left, hence the left boundary condition $\eta(0,\tau) = 1.5$ for $\tau > 0$. It shows that a sudden discharge travels to the right with phase velocity

$$\frac{[G(\eta)]}{[\eta]} = \frac{1.5^{3/2}-1}{0.5} = 1.67. \quad (14)$$

Fig.3 clearly shows that our numerical model can simulate the evolution of a step function wave with the correct speed.

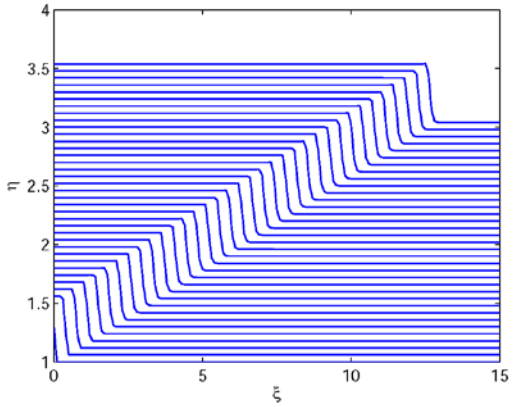

Fig.3 Simulation of uniform flow for $0 < \tau < 74$. An incoming sudden discharge with height $\bar{a} = 0.5$ flows from the left with phase velocity 1.6742.

4.2 Subcritical and Supercritical Flows over a Bump

In this simulation setup, a bump is placed at a specified interval on the bottom, and flat for other so that the surface waves can be generated. In the first simulation, we will compare our result against the result presented in [1] which is obtained using Boussinesq-type model to validate our model. For numerical computation, we use $w(x,0) = 1$, the left boundaries is $w(0,t) = 1$ representing the situation of uniform that is far from the disturbance. Meanwhile, the right boundaries are set by absorbing boundary. First, we observe flow over a bump on flat bottom with $\theta = 0$. The bump is generated by a function below, following the

function that is used in [1].

$$b(x) = 0.18sech^2(0.3(x-100)).$$

The comparison is presented in Fig. 4, where we plot $\eta(x,40)$ for $F = 1.5$ of both SWE model and Boussinesq model. The figure shows that our model confirms the result obtained using Boussinesq-type model.

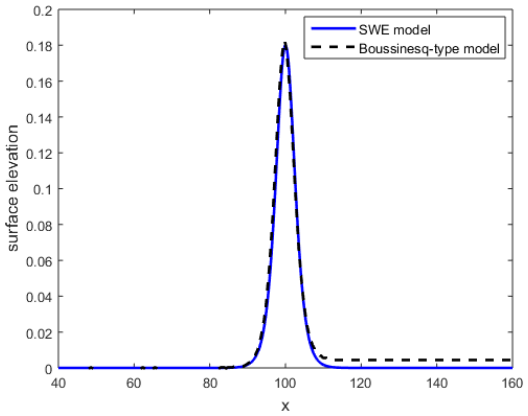

Fig.4 Comparison of $\eta(x,40)$ obtained using SWE model and Boussinesq-type model on flat bottom ($\theta = 0$) with bump for $F = 1.5$.

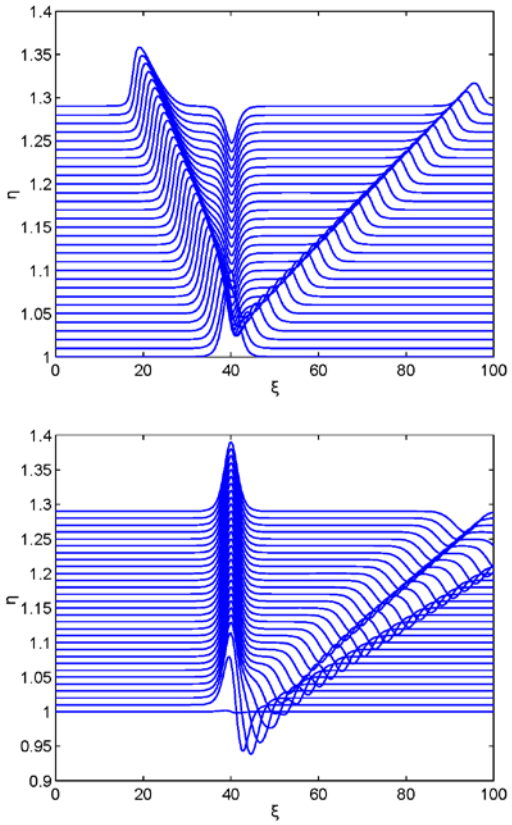

Fig.5 Free-surface profile of flow over a secant-hyperbolic-bump on flat bottom ($\theta = 0$), for $F = 0.4$ (upper) and $F = 1.4$ (lower), without diffusive terms $1/Re = 0$.

Further, the characteristic of the flow over a bump with different value of Froude number will be investigated. Fig.5 is typical solution of Eq. (3,4) for subcritical flow ($F < 1$) and a very large Reynolds number $Re \to \infty$. We plot some free surfaces η by shifting upward for different larger value τ. The plot is the result of calculation for $F = 0.4$ and $F = 1.4$. The flow is disturbed by a bump of secant-hyperbolic function

$$b(x) = 0.1sech^2(0.5(x-40)).$$

The free surface fluid over the bump forms wave that grows, splits at the same time propagates to the left, right and remain above the bump. For the subcritical flow, the positive elevation spreads to the left and right, and one of the negative-amplitude waves stays above the bump. Otherwise, for supercritical flow, the disturbance of the flow causes the surface is lifted up, and increasing the height above the bump, as shown in Fig.5 (lower), followed by propagating the wave, which is generated two waves on the right side of the bump.

Next, we consider the diffusive terms with a certain value of Re. The effect of the Reynolds number can be seen on wave damping in a free surface, see Fig. 6. Smaller Reynolds numbers give us larger damping.

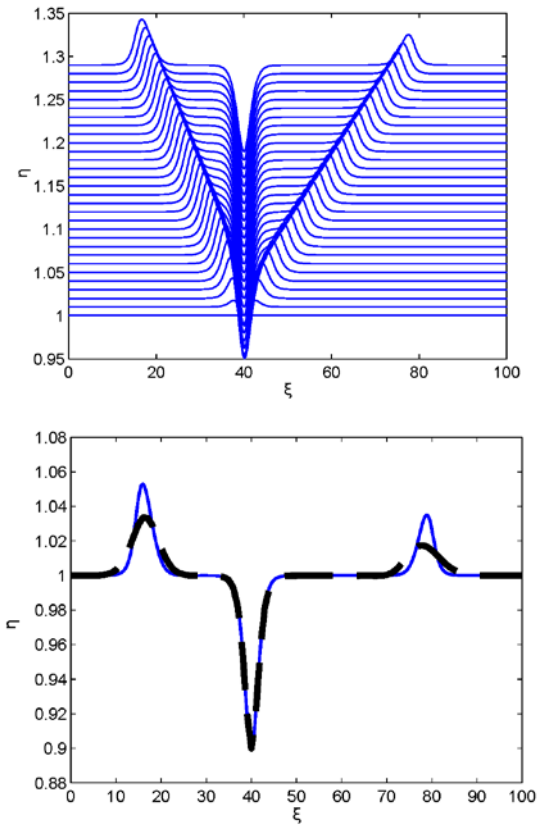

(a)

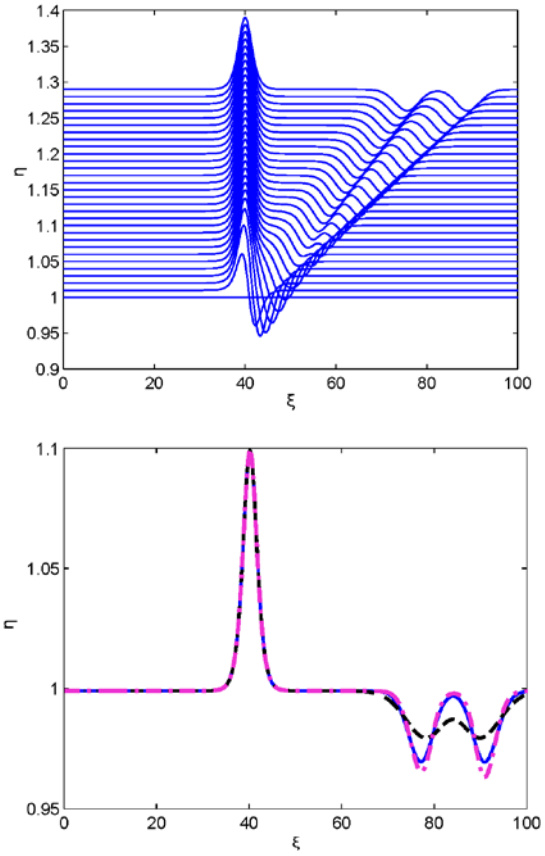

(b)

Fig.6 Plot of $\eta(\xi, 15)$ for (a) $F = 0.4$ (b) $F = 1.4$ and different Reynolds number. Dash line, solid, and dash dotted is for $Re = 1{,}50$, and 1000, respectively.

Plots of the free surface resulting from the similar calculation above are shown in Fig. 4 using different Reynold number. Fig.6(a) is for subcritical flow and 6(b) for supercritical flow. We run for $Re = 1$ and $Re = 50$. The surface $\eta(\xi, 15)$ related to Fig. 5 ($Re = 50$) is similar to Fig. 6, but with reduction in the amplitude.

4.3 Flows over a Bump on an inclined Channel

Experimentally, it has been proved that undular bores or secondary waves appear when the flow has a Froude number in the range between 1 and 1.7 [14]. Not all numerical scheme can simulate this phenomenon. In this subsection, we implement our numerical scheme to simulate wave generation over a bump on an inclined channel with $\theta = \pi/18$ for supercritical flow. For computation, we use the same setup that is chosen above. In the case of supercritical flow $F = 1.4 > 1$, it can be seen in Fig.7 the appearance of secondary waves that we called undular bores where we could not find in subcritical flow.

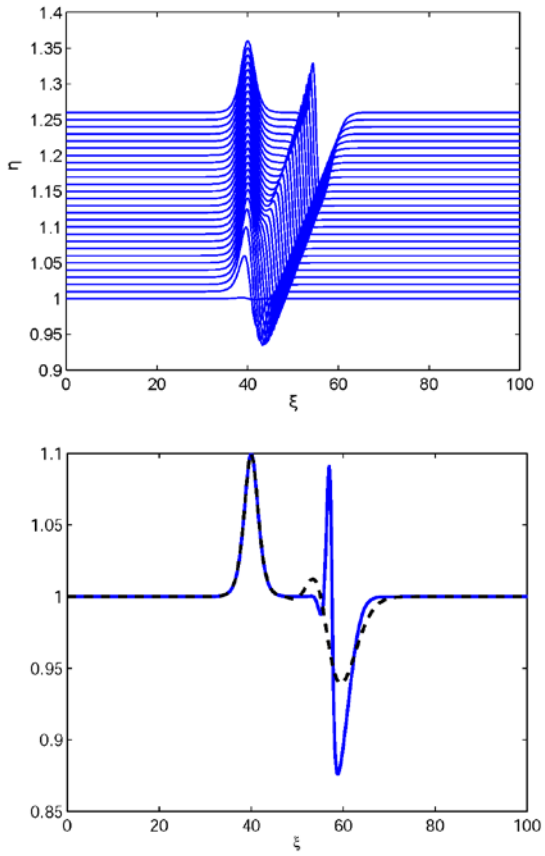

Fig.7 (upper) Surface profile $\eta(\xi, \tau)$ for $F = 1.4$. (lower) Profile of $\eta(\xi, 15)$ with different Reynolds number, Dash line: $Re = 1$, solid line: $Re = 50$.

A numerical scheme over a different type of obstruction is also implemented. This simulation is aimed to study about the dependence of the free surface wave formed by a bump. The obstruction is a cosine bump that is written as

$$\boldsymbol{b(x) = 0.1\cos\left(\frac{\pi}{15(x - 3\pi)}\right)}$$

$$\boldsymbol{for\ 32.5 < x < 42.5}$$

and zeros value for elsewhere x. Here, the same parameters are used that was applied above with $Re = 50$. As we saw in Fig.8, the generation of free surface over a cosine bump is also a kind of cosine form. In all previous test cases, the free surface waves over a bump is a kind of secant hyperbolic function as same as the bump form. Further, we can see that the cosine bump generates secondary waves more, see Fig.8 (lower).

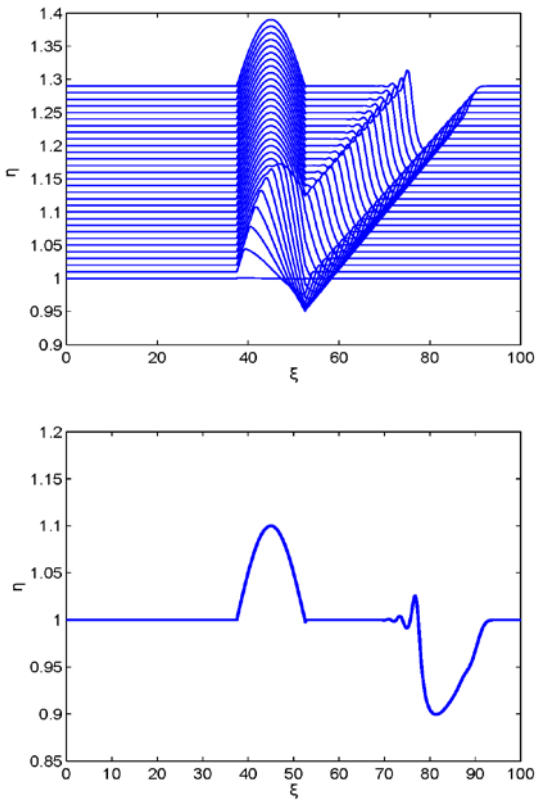

Fig.8 (upper) Surface profile $\eta(\xi,\tau)$ for several time. (lower) Profile of $\eta(\xi,15)$ including the appearance of undular bores.

5. CONCLUSION

The Shallow Water Equation governs the evolution of wave down an inclined channel with a bump. A staggered finite method is applied to solve the full nonlinear equation numerically. In the uniform flow case, the numerical scheme can produce the propagation of a step function with the correct speed. Further, the scheme can simulate the evolution of flow over a bump on an inclined channel for various Froude and Reynold numbers. Different Reynold number gives us the different value of damping. Moreover, the appearance of secondary waves is successfully produced by our numerical scheme appear in case of an inclined channel. And it depends on the form of the bump.

6. ACKNOWLEDGEMENTS

This work was supported by Riset Terapan and PDUPT Grant.

7. APPENDIX

From the sketch of the flow and coordinates Figure 1, we take a small fluid element $\boldsymbol{x} \in [\boldsymbol{x_1}, \boldsymbol{x_2}]$. The mass conservation of fluid for that element can be written

$$\frac{\boldsymbol{d}}{\boldsymbol{dt}}\int_{x_1}^{x_2}(\boldsymbol{h}-\boldsymbol{d})\boldsymbol{dx}+\left((\boldsymbol{h}-\boldsymbol{d})\boldsymbol{u}|_{x_1}^{x_2}\right)=\boldsymbol{0}$$

and the momentum conservation

$$\frac{\boldsymbol{d}}{\boldsymbol{dx}}\int_{x_1}^{x_2}(\boldsymbol{h}-\boldsymbol{d})\boldsymbol{udx}+\left((\boldsymbol{h}-\boldsymbol{d})\boldsymbol{u}^2|_{x_1}^{x_2}\right)+\left(\frac{\boldsymbol{1}}{\boldsymbol{2}}\boldsymbol{g}(\boldsymbol{h}-\boldsymbol{d})^2\boldsymbol{\cos\theta}|_{x_1}^{x_2}\right)=\int_{x_1}^{x_2}\boldsymbol{g}(\boldsymbol{h}-\boldsymbol{d})\boldsymbol{\sin\theta dx}-\int_{x_1}^{x_2}\boldsymbol{C_f u^2 dx}.$$

Since those equations are valid for any fluid element, we can write in

$$\frac{\boldsymbol{\partial h}}{\boldsymbol{\partial t}}=-\frac{\boldsymbol{\partial}}{\boldsymbol{\partial x}}((\boldsymbol{h}-\boldsymbol{d})\boldsymbol{u})$$

$$\frac{\boldsymbol{\partial}}{\boldsymbol{\partial t}}((\boldsymbol{h}-\boldsymbol{d})\boldsymbol{u}^2)+\frac{\boldsymbol{1}}{\boldsymbol{2}}\boldsymbol{g\cos\theta}\frac{\boldsymbol{\partial}}{\boldsymbol{\partial x}}((\boldsymbol{h}-\boldsymbol{d})^2)=\boldsymbol{g\sin\theta}(\boldsymbol{h}-\boldsymbol{d})-\boldsymbol{C_f u^2}.$$

The second equation is then expanded and we use the first one to simplify the equation. Meanwhile, we include the effect of the energy dissipation by shearing normal to the flow which is proportional to the second derivation of the velocity. So that the second equation becomes

$$\frac{\boldsymbol{\partial u}}{\boldsymbol{\partial t}}+\boldsymbol{u}\frac{\boldsymbol{\partial u}}{\boldsymbol{\partial x}}+\boldsymbol{g\cos\theta}\left(\frac{\boldsymbol{\partial h}}{\boldsymbol{\partial x}}-\frac{\boldsymbol{\partial d}}{\boldsymbol{\partial x}}\right)=\boldsymbol{g\sin\theta}-\boldsymbol{C_f}\frac{\boldsymbol{u^2}}{\boldsymbol{h}-\boldsymbol{d}}+\boldsymbol{\nu_0}\frac{\boldsymbol{\partial^2 u}}{\boldsymbol{\partial x^2}}$$

with ν_0 as the proportional constant, physically as the eddy viscosity.

8. REFERENCES

[1] Wiryanto L., and Mungkasi S., A boussinesq-type model for waves generated by flow over a bump. Applied Mathematical Sciences, Vol. 8, Issue 106, 2014, pp.5293-5302.

[2] Shen S.P., Shen M.C., and Sun S.M., A model equation for steady surface waves over a bump. Journal of Engineering Mathematics, Vol. 23, Issue 4, 1989, pp.315-323.

[3] Wiryanto L., and Jamhuri M., Supercritical flow generating a solitary-like wave above a bump. Journal on Industrial and Applied Mathematics, Vol. 2, Issue 1, 2015, pp.1-8.

[4] Whitham G., Linear and Nonlinear Waves. Pure and Applied Mathematics: A Wiley Series of Texts, Monographs and Tracts. Wiley, New Jersey, United States, 2011.

[5] Wiryanto L., Flow on an inclined open channel. Nonlinear Analysis and Differential Equations, Vol. 4, Issue 11, 2016, pp.541-547.
[6] Dressler R.F., Mathematical solution of the problem of roll-waves in inclined opel channels. Communications on Pure and Applied Mathematics, Vol. 2, Issue 2-3, 1949, pp.149-194.
[7] Needham D.J., and Merkin J.H., On roll waves down an open inclined channel. Proceedings of the Royal Society of London. Series A, Mathematical and Physical Sciences, Vol. 394, Issue 1807, 1984, pp.259-278.
[8] Que Y.T., and Xu K., The numerical study of roll-waves in inclined open channels and solitary wave run-up. International Journal for Numerical Methods in Fluids, Vol. 50, Issue 9, 2006, pp.1003-1027.
[9] Stoker J., Water waves: The mathematical theory with applications. Wiley, New Jersey, United States, 1958.
[10] Pudjaprasetya S., and Magdalena I., Momentum conservative schemes for shallow water flows. East Asian Journal on Applied Mathematics, 4, Issue 2, 2014, pp.152-165.
[11] Magdalena I., Pudjaprasetya S.R., and Wiryanto, L.H., Wave interaction with an emerged porous media. Advances in Applied Mathematics and Mechanics, Vol. 6, Issue 5, 2015, pp.680-692.
[12] Magdalena I., Erwina N., and Pudjaprasetya S., Staggered momentum conservative scheme for radial dam break simulation. Journal of Scientific Computing, Vol. 3, Issue 65, 2015, pp.867-874.
[13] Magdalena I., Non-hydrostatic model for solitary waves passing through a porous structure. Journal of disaster research, Vol. 11, Issue 5, 2016, pp.957-963.
[14] Koch C., and Chanson H., Turbulent mixing beneath an undular bore front. Journal of Coastal Research, Vol. 24, Issue 4, 2008, pp.999-1007.